ESRF	**Experiment title:** **Localisation of deformation mechanisms and damage in Ti alloys**	**Experiment number**:
Beamline: ID19	**Date of experiment**: from: 4 July 2008 to: 7 July 2008	**Date of report**: 26Aug 2009
Shifts: 9	**Local contact(s)**: Peter Cloetens	*Received at ESRF:* *27 Aug 2009*

Names and affiliations of applicants (* indicates experimentalists):

Guillermo Requena[1*]

Hans Peter Degischer[1*]

Cecilia Poletti[1*]

Fernando Warchomicka[1*]

Domonkos Tolnai[1*]

Michael Schöbel[1*]

Report:

Room temperature holotomography of Ti6Al6V2Sn (Ti662) and Ti10V2Fe3Al (Ti1023) titanium alloys was carried out at the ID19. The alloys were investigated in as received condition and after different high temperature compression tests. The investigated conditions are summarized in Table 1. The voxel size for the tomographies was selected according to the expected size of microstructural features of the alloys.

Alloy	Strain rate [1/s]	Temperature [°C]	Strain	Voxel size
Ti662 powder metallurgy	As received			$(0.7\ \mu m)^3$
Ti662 powder metallurgy	1	850	0.5	$(0.7\ \mu m)^3$
			0.6	$(0.7\ \mu m)^3$ - $(0.3\ \mu m)^3$
Ti662 ingot	0.1	650	0.4	$(0.7\ \mu m)^3$
			0.6	$(0.7\ \mu m)^3$ - $(0.3\ \mu m)^3$
Ti1023	- non deformed -	740°C / 30min	-	$(0.7\ \mu m)^3$
Ti1023	50	740	0.7	$(0.3\ \mu m)^3$
Ti1023	0.001	740	0.7	$(0.3\ \mu m)^3$

Table 1. Investigated alloys and their corresponding conditions.

The parameters used for the tomographic scans are shown in Table 2. Three different sample-detector distances were used in order to perform effective phase retrieval. This was necessary due to the low absorption contrast between the phases of the investigated alloys. Portions of the holotomographic reconstructions are shown in Fig. 1 to Fig. 4 for all the investigated alloys and conditions.The $(0.7\ \mu m)^3$ voxel size was enough to resolve the alpha and beta phases of the Ti662 alloys as well as some porosity due to the processing in the powder metallurgy Ti662 alloy (see Fig. 1a). On the other hand, only grain

boundaries could be resolved for the Ti1023 alloy with the $(0.3\mu m)^3$ and $(0.7\mu m)^3$ voxel sizes (see Fig. 1b and Fig. 4).

Voxel Size	Beam energy [keV]	Distance sample-detector [mm]	Nr. of radiographies
$(0.3\ \mu m)^3$	29	5 – 11 – 39	1500
$(0.7\ \mu m)^3$	40	5 – 32 – 91	1200

Table 2. Parameters used for the tomographic scans.

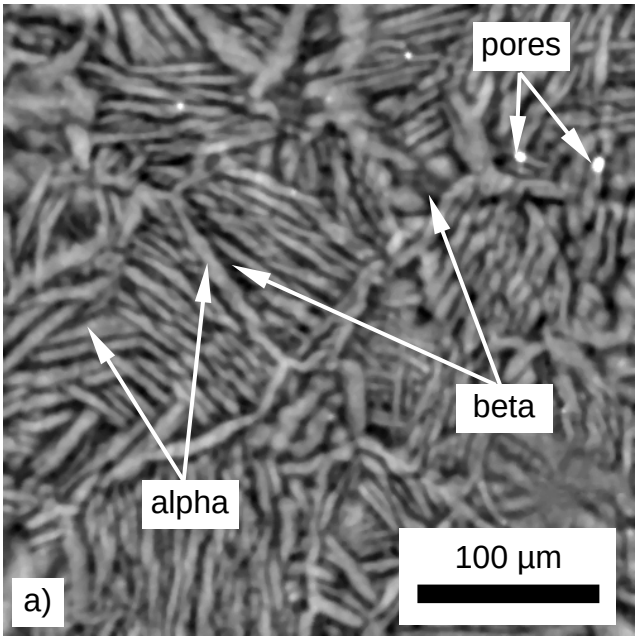

Fig. 1. a) **Ti662PM AR** $(0.7\ \mu m)^3$

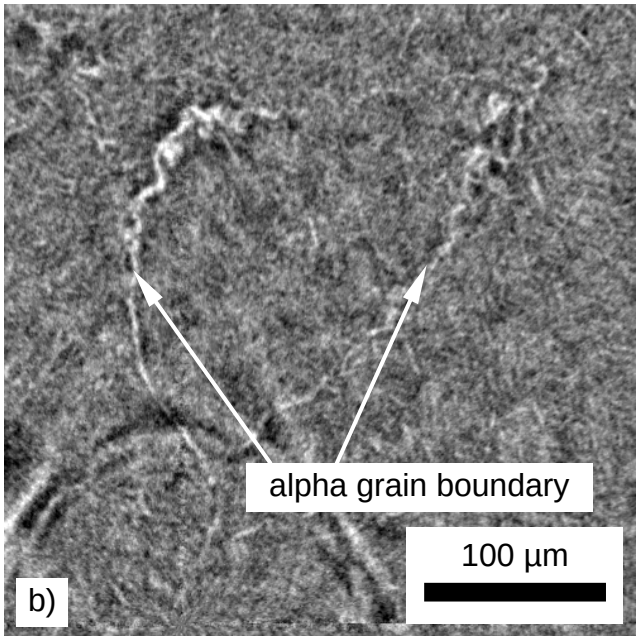

b) **Ti1023 not deformed** $(0.7\ \mu m)^3$

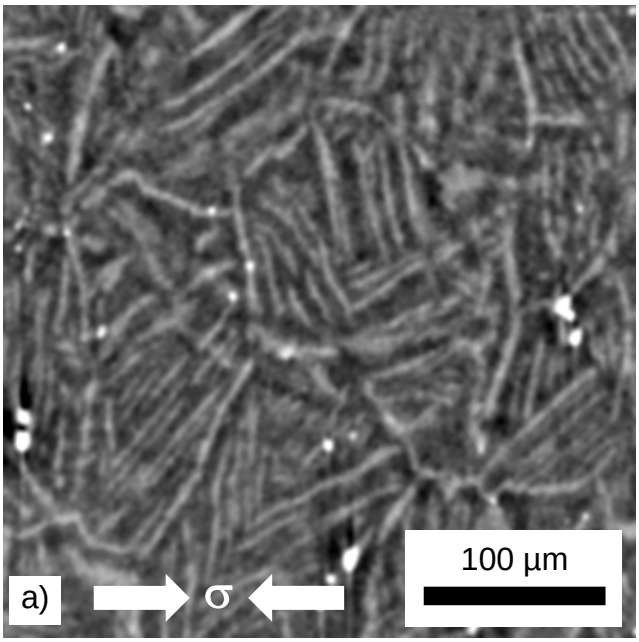

Fig. 2. a)**Ti662 PM** 1 s^{-1} 850°C 0.5 $(0.7\ \mu m)^3$

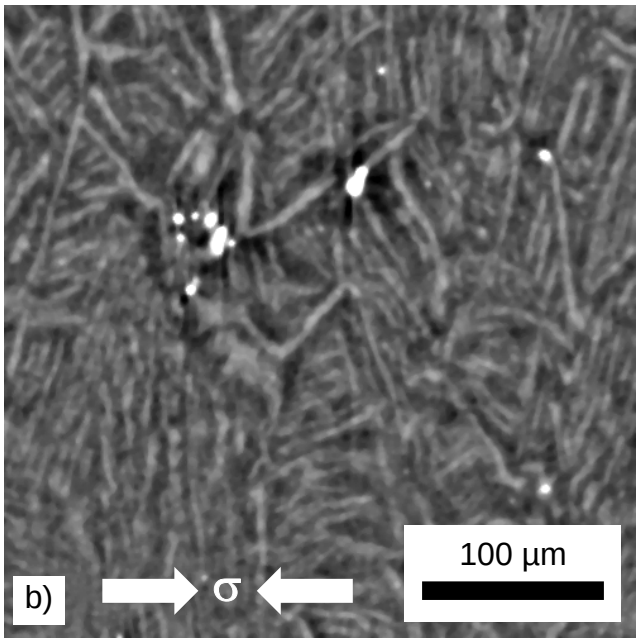

b) **Ti662 PM** 1 s^{-1} 850°C 0.6 $(0.7\ \mu m)^3$

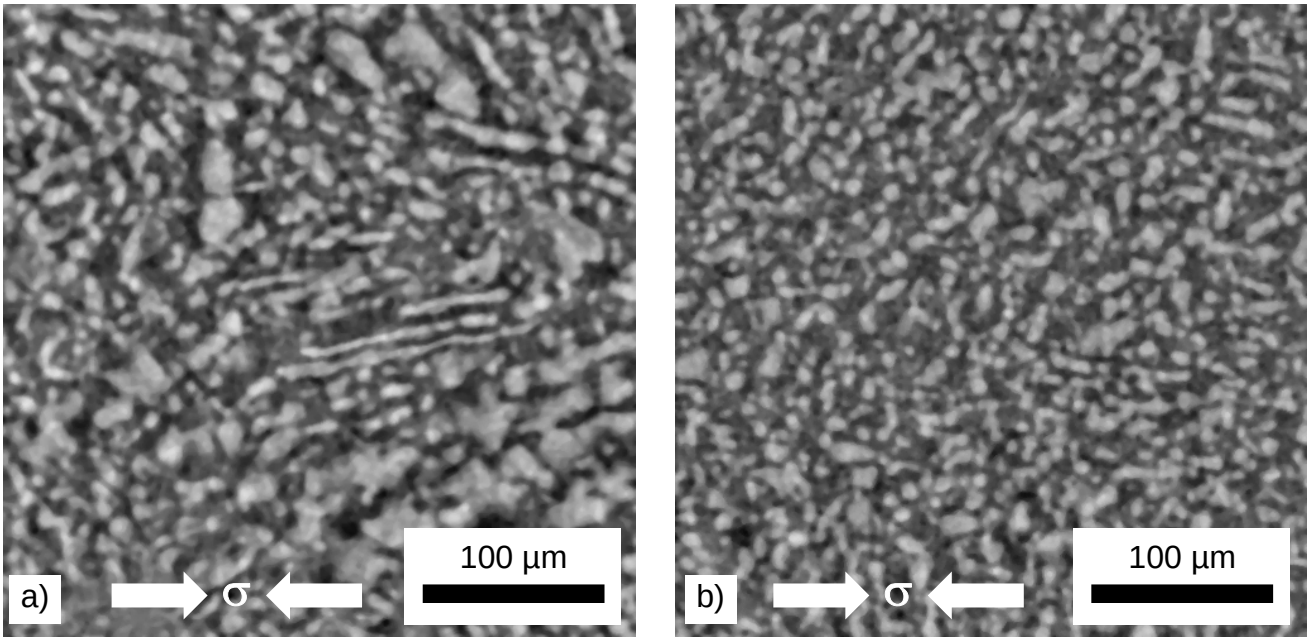

Fig. 3. a) **Ti662 ingot** 0.1 s^{-1} 650°C 0.4 $(0.7\ \mu m)^3$ b) **Ti662 ingot** 0.1 s^{-1} 650°C 0.6 $(0.7\ \mu m)^3$

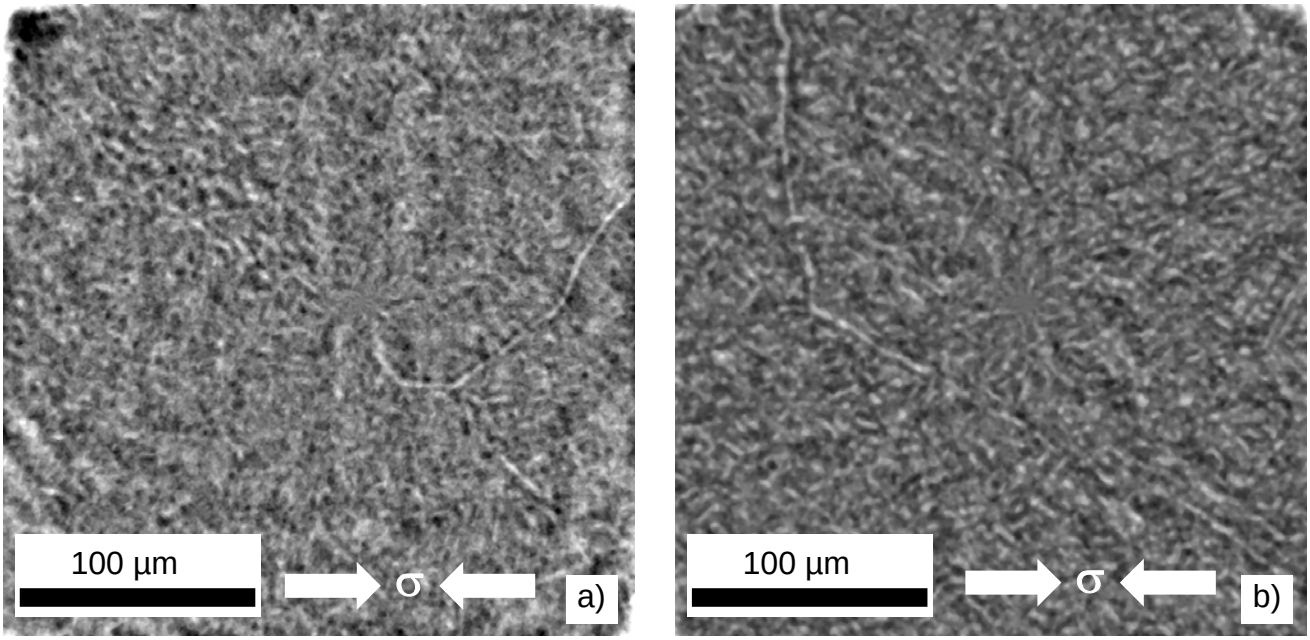

Fig. 4. a) Ti1023 50 s^{-1} 740°C 0.7 $(0.3\ \mu m)^3$ b)Ti1023 0.001 s^{-1} 740°C 0.7 $(0.3\ \mu m)^3$

Fig. 5 shows an example of a reconstructed holotomographic slice with voxel size $(0.3\ \mu m)^3$ for the Ti662 alloy produced by powder metallurgy and deformed at 850°C with a deformation rate of 1 s^{-1} to a final strain of 0.6. Zones with deformed alpha lamellae and cracks going through some of the alpha lamellae are indicated. The identification of these different deformation mechanisms was the objective of the experiment. The use of holotomography has shown to result in effective phase retrieval to resolve the microstructural features of most of the investigated materials. The currents status of the work is focused on the 3D identification of the possible deformation mechanisms and its correlation with experimental flow data for the studied materials and conditions.

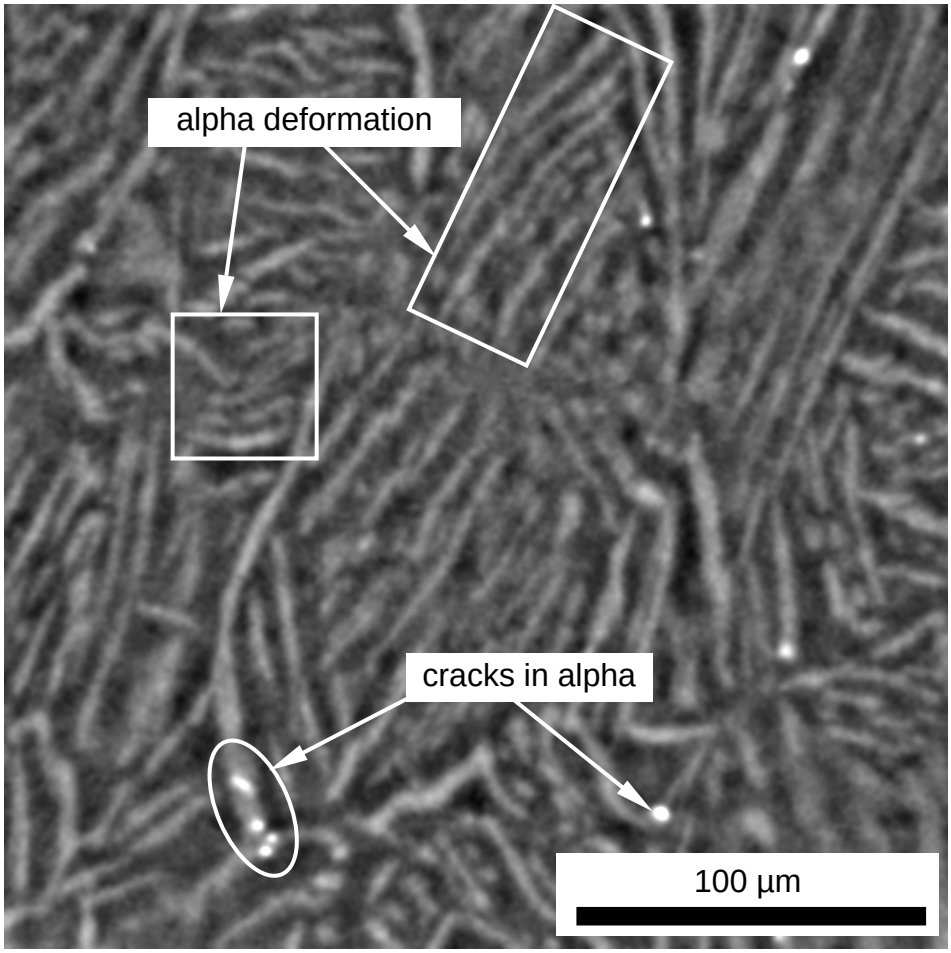

Fig. 5. **Ti662 PM** 1 s^{-1} 850°C 0.6 (0.3 µm)³